Supporting Information

Pharmaceutical Crystalline Complexes of Sulfamethazine with Saccharin: Same Interaction Site but Different Ionization States

Xue Fu,[†,‡] Jianhui Li,[‡] Lianyan Wang,[‡] Bing Wu,[§] Xu Xu,[*,†] Zongwu Deng[‡] and Hailu Zhang[*,‡]

[†] School of Chemical and Environmental Engineering, Shanghai Institute of Technology, Shanghai 201408, P.R. China.

[‡] Laboratory of Magnetic Resonance Spectroscopy and Imaging, Suzhou Institute of Nano-Tech and Nano-Bionics, Chinese Academy of Sciences, Suzhou 215123, P.R. China.

[§] Analysis and Testing Center, Soochow University, Suzhou 215123, P.R. China.

---

[*] Corresponding Authors:

E-mail: hlzhang2008@sinano.ac.cn; Tel: +86-512-62872713; Fax: +86-512-62603079. (HLZ)

E-mail: xuxu@sit.edu.cn; Tel: +86-20-60873372. (XX)

1 Materials and methods

1.1 Materials and sample preparation

SMT (≥99%) and SAC (≥99%) were purchased from Aladdin Industrial Inc. (Shanghai, China) and Alfa Aesar (Shanghai, China), respectively. Ultrapure water was used throughout the experiments. Other chemicals used were of analytical grade and used as received without any further purification.

SMT (27.8 mg, 0.1 mmol) and SAC (18.3 mg, 0.1mmol) were dissolved in different solvents (methanol/water, methanol/acetonitrile, methanol, acetone, acetonitrile, chloroform, ethanol, dichloromethane, isopropanol) and then filtered through 0.22 μm PTFE syringe filter. Each resulting solution was left to slowly evaporate at room temperature. Generally, colorless crystals were harvested after 1–3 weeks. In most experimental condition (except acetone and dichloromethane), satisfied single-crystal samples can be easily obtained.

1.2 Characterization

1.2.1 Single-crystal X-ray diffraction (SXRD): SXRD data were obtained using a Agilent Gemini Atlas diffractometer (Agilent, Santa Clara, California) with graphite-monochromated Mo Kα radiation (λ = 0.71073 Å) for SMT-SAC salt and Cu X-ray source (λ = 1.54184 Å) for SMT-SAC cocrystal. The data were collected at 220 K for both. The X-ray generator was operated at 40 kV and 40 mA and the X-ray data collection was monitored by the *CrysAlisPro* program. Cell parameters were refined on all observed reflections by using the program *CrysAlisPro* (Agilent Technologies, Version 1.171.36.32, 2013). The crystal structures of both forms were solved by direct methods and refined on F^2 by full-matrix least-squares techniques with *SHELXTL-97* program.[1] A full-matrix leastsquares refinement was used for the non-hydrogen atoms with anisotropic thermal parameters. Hydrogen atoms associated with carbon atoms were fixed in geometrically constrained positions. The hydrogen atoms on the N atoms were located from the difference Fourier map with their N–H distances restrained to N–H = 0.80 Å and thermal parameters constrained to $U_{\mathrm{iso}}(\mathrm{H}) = 1.2U_{\mathrm{eq}}(\mathrm{N})$. All non-hydrogen atoms in the salt and cocrystal were refined anisotropically. All the calculations were performed on a Dell workstation using the *Olex2* crystallographic software package.[2] X-ray crystallographic data are listed in Table S1, and geometrical parameters of hydrogen bonds are provided in Table S4.

1.2.2 Powder X-ray diffraction (PXRD): PXRD measurements were conducted on a Brucker D8 advance X-ray power diffractometer (Bruker AXS, Karlsruhe, Germany) equipped with a LynxEye detector. A Cu Kα radiation was used at 45 kV and 40 mA. Samples were scanned in the reflection mode from 3 to 40° 2θ with a scanning step size of 0.01° and a counting time per step of 8.8 s.

1.2.3 Differential Scanning Calorimetry (DSC): DSC experiments were carried out using a TA Q2000 differential scanning calorimeter (TA Instruments, New Castle, DE) with scan rate of 10 °C/min under nitrogen atmosphere.

1.2.4 Solid state NMR: ^{13}C Cross-Polarization/Magic Angle Spinning (CP/MAS) NMR experiments were performed with a 4-mm double-resonance MAS probe on a Bruker AVANCE III-500 spectrometer (Bruker BioSpin, Karlsruhe, Germany) operating at a magnetic field strength of 11.7 T. A total sideband suppression (TOSS) frame was embedded into the conventional CP pulse sequence. The ^{13}C NMR spectra were obtained at 8 kHz MAS spinning speed with a 2 ms contact time and 8 s recycle delay. ^{13}C chemical shift was externally referenced to tetramethylsilane (TMS, 0 ppm).

1.3 Energy calculations for SMT-SAC ionic/molecular pairs

The initial SMT-SAC pairs were taken from salt and cocrystal structures, respectively. Additionally, ionization state was also artificially modified for each pair. Geometry optimizations and single point energy calculations were performed with GAUSSIAN program suite with DFT method (B3LYP functional, 6-311++G (d, p) basis set). Calculations on relative orientation (of the two rings of SMT) fixed models were also carried out. The relative orientation was fixed by freezing the dihedral angle N3–N4–S1–C1 and dihedral angle N4–S1–C1–C6.

1.4 Geometry optimizations, single point energy calculations, and theoretical chemical shifts calculations for the periodic structural models

The SMT-SAC salt and SMT-SAC cocrystal structures were subjected to geometry optimization and NMR shielding calculation by using *MS CASTEP* program. Calculations were carried out by using the generalized gradient approximation (GGA), Perdew-Burke-Ernzerhof (PBE) functional with the Grimme dispersion correction. The optimization (and single point energy calculation) was carried out with an energy cutoff of 300 eV, ultrasoft pseudopotential and default K-point setting. While in the NMR shielding calculation, a fine

K-point and energy cut-off of 550 eV were employed, combining with core-valance interactions described by ultrasoft pseudopotential generated on-the-fly.

1.5 Solubility and stability study

Saturation solubility studies of SMT-SAC salt and SMT-SAC cocrystal were carried out in water. Each sample equivalent to 50 mg of SMT was added to the screw-capped test tubes with 5 mL of ultrapure water. The oversaturated suspension was treated at 25 ± 0.5 °C & 37 ± 0.5 °C in an incubator shaker rotating at 120 rpm. After 72 h, the solutions were filtered through 0.22 μm polycarbonate filter and their concentrations were detected by Waters HPLC system (Waters2535) equipped with PDA detector at 242.6 nm. Each determination was performed in triplicate and the remaining solids were verified by PXRD measurements to monitor possible transformation.

To investigate the stability of the crystalline complexes, excessive amounts of SMT-SAC salt or SMT-SAC cocrystal was stirred in water, acetonitrile, or dichloromethane for 72 h at room temperature. Also, SMT-SAC salt and SMT-SAC cocrystal were placed at 95% Relative Humidity (RH)/25°C for two weeks. Solids were subjected to PXRD measurements to monitor possible solid-form transformation.

1.6 Rietveld refinement.

Powder Refinements were performed to confirm the structural agreement of single crystal sample and bulk sample. For salt or cocrystal, the experimental PXRD pattern and the determined crystal structure were imported into Materials Studio software. Powder Refinement tool was employed with a middle convergence quality. Range of 2-Theta and Radiation values were set according to the experimental parameters for the PXRD measurement. Pseudo-Voigt peak profile was used, and FWHM, Profile, Line shift and Asymmetry parameters of pattern were refined. The fractional coordinates of a structure were fixed during lattice changes. Finally, sample preferred orientation was refined using same convergence quality.

1 (a) G. M. Sheldrick, *SHELXS-97, Program for Solution of Crystal Structures*, University of Göttingen, Göttingen, Germany, 1997; (b) G. M. Sheldrick, *SHELXL-97, Program for Refinement of Crystal Structures*, University of Göttingen, Göttingen, Germany, 1997.

2 O. V. Dolomanov, L. J. Bourhis, R. J. Gildea, J. A. K. Howard and H. Puschmann, *J. Appl. Crystallogr.*, 2009, 42, 339.

Table S1 X-ray crystallographic data for SMT-SAC salt and SMT-SAC cocrystal

	Salt	Cocrystal
Formula	$C_{19}H_{19}N_5O_5S_2$	$C_{19}H_{19}N_5O_5S_2$
Crystal system	Orthorhombic	Monoclinic
Space group	*Pbca*	$P2_1/n$
a/Å	10.5425(3)	8.0729(3)
b/Å	16.0431(4)	17.6015(7)
c/Å	25.3246(6)	14.4311(6)
α/°	90	90
β/°	90	104.488(4)
γ/°	90	90
Volume/Å³	4283.2(2)	1985.40(13)
Z/Z′	8/1	4/1
T	220 K	220 K
D_{calc} (g cm^{-3})	1.431	1.544
F(000)	1920	960
R_{int}	0.0330	0.0410
Reflns collected	21676	7165
Unique reflns	4376	3553
Observed reflns	3426	2853
Number parameters	305	294
Absorption coeff (mm^{-1})	0.290	2.830
Crystal size (mm)	0.4×0.3×0.15	0.3×0.05×0.05
GOF on F^2	1.013	1.051
$R_1[I > 2\sigma(I)]/R_1$	0.0398/0.0559	0.0473/0.0607
$wR_2[I > 2\sigma(I)]/wR_2$	0.1283/0.1428	0.1185/0.1302
CCDC	1437001	1416185

Table S2 The calculated and experimental ^{13}C chemical shifts for the actual existed SMT-SAC salt and SMT-SAC cocrystal structures, and their possible isomers.

SMT-SAC salt			SMT-SAC cocrystal		
Position	δ_{cal}	δ_{exp}	Position	δ_{cal}	δ_{exp}
C1	122.62	123.56	C1	132.09	131.54
C2	128.31	130.58	C2	126.46	128.28
C3	115.41	115.43	C3	115.77	117.14
C4	152.38	154.20	C4	152.32	155.22
C5	110.94	111.98	C5	115.52	116.48
C6	132.21	133.66	C6	124.14	124.13
C7	145.89	150.24	C7	150.58	152.79
C8	160.54	164.25	C8	155.16	159.45
C9	111.82	114.53	C9	109.53	111.47
C10	171.24	174.71	C10	174.11	177.97
C11	17.99	20.17	C11	19.47	21.08
C12	27.56	26.73	C12	26.51	26.87
C1'	120.64	122.32	C1'	123.03	123.33
C2'	131.57	131.71	C2'	136.81	138.11
C3'	132.71	134.18	C3'	139.77	139.28
C4'	120.46	120.10	C4'	124.59	126.90
C5'	143.40	142.17	C5'	136.80	135.47
C6'	130.84	130.58	C6'	123.68	125.76
C7'	171.60	171.09	C7'	164.08	165.82
Virtual neutral isomer of SMT-SAC salt			Virtual ionic isomer of SMT-SAC cocrystal		
C1	127.14	123.56	C1	129.13	131.54
C2	128.02	130.58	C2	128.16	128.28
C3	114.04	115.43	C3	116.30	117.14
C4	151.92	154.20	C4	153.37	155.22
C5	110.35	111.98	C5	116.27	116.48
C6	131.99	133.66	C6	125.25	124.13
C7	149.31	150.24	C7	147.39	152.79
C8	156.43	164.25	C8	158.84	159.45
C9	107.05	114.53	C9	114.59	111.47
C10	173.64	174.71	C10	174.40	177.97
C11	17.68	20.17	C11	20.46	21.08
C12	28.35	26.73	C12	26.49	26.87
C1'	123.68	122.32	C1'	121.41	123.33
C2'	135.94	131.71	C2'	134.16	138.11
C3'	137.57	134.18	C3'	137.13	139.28
C4'	121.00	120.10	C4'	123.15	126.90
C5'	138.59	142.17	C5'	142.68	135.47
C6'	125.09	130.58	C6'	129.37	125.76
C7'	166.42	171.09	C7'	171.46	165.82

Table S3 Values of dihedral angles N3–N4–S1–C1 and N4–S1–C1–C6 before and after optimization at B3LYP /6-311++G (d, p) level without freezing the relative orientation of the two rings of SMT.

	N3–N4–S1–C1		N4–S1–C1–C6	
Model (Fig. 4)	Before	After	Before	After
a	67.04°	73.43°	96.73°	106.79°
b	67.04°	70.29°	96.73°	100.23°
c	60.12°	70.93°	154.82°	99.15°
d	60.12°	74.34°	154.82°	105.36°

Table S4 Geometrical parameters of hydrogen bonds in SMT-SAC salt and SMT-SAC cocrystal

D-H···A	D···H (Å)	H···A(Å)	D···A (Å)	D—H···A (deg)
SMT-SAC Salt				
N(2)—H···O(1’)	0.88	1.75	2.626(2)	171
$N(4)^+$—H···$N(1')^-$	0.84	1.95	2.782(2)	176
N(1)—H···O(2)	0.834	2.158	2.972(3)	165
N(1)—H···O(1)	0.816	2.220	3.029(3)	171
C(6)—H···O(2)	0.93	2.65	2.970(3)	101.0
C(2)—H···O(1)	0.93	2.59	2.935(3)	102.4
C(1’)—H···O(1’)	0.93	2.83	3.011(3)	92.0
SMT-SAC Cocrystal				
N(2)—H···O(1’)	0.83	1.95	2.778(3)	177
N(1’)—H···N(4)	0.89	2.04	2.919(3)	174
N(1)—H···O(1)	0.88	2.31	3.156(4)	160
N(1’)—H···O(2)	0.879	2.653	3.253	126.42
C(6)—H···O(1)	0.93	2.59	2.926(4)	101.5
C(2)—H···N(4)	0.93	2.77	3.128(4)	103.8

Table S5 The saturation solubilities of SMT-SAC salt and SMT-SAC cocrystal.

Sample	Saturation solubility (mg/ml)	
	25°C	37°C
SMT-SAC salt	1.88	2.17
SMT-SAC cocrystal	1.70	1.87

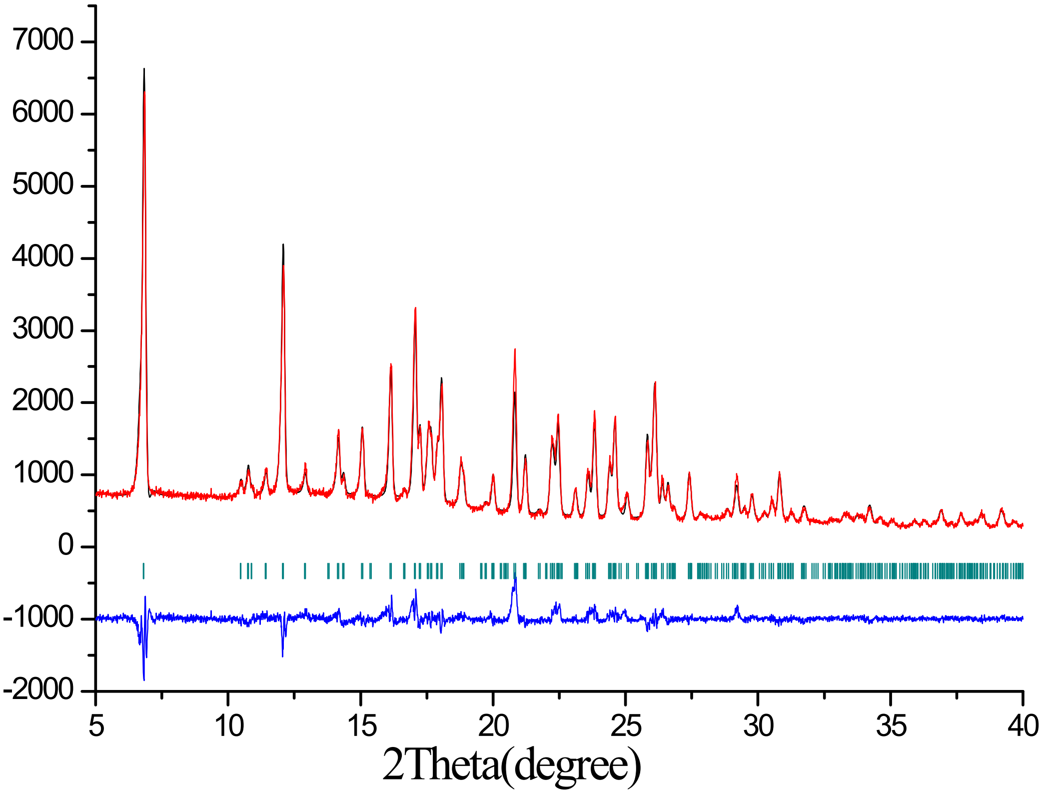

Figure S1 Experimental PXRD pattern (red), Rietveld simulated PXRD pattern (black) and their difference profile (blue) of SMT-SAC salt. The observed reflections are also marked (darkcyan). Residual variances: *R*wp = 6.76%, *R*p = 5.10 %.

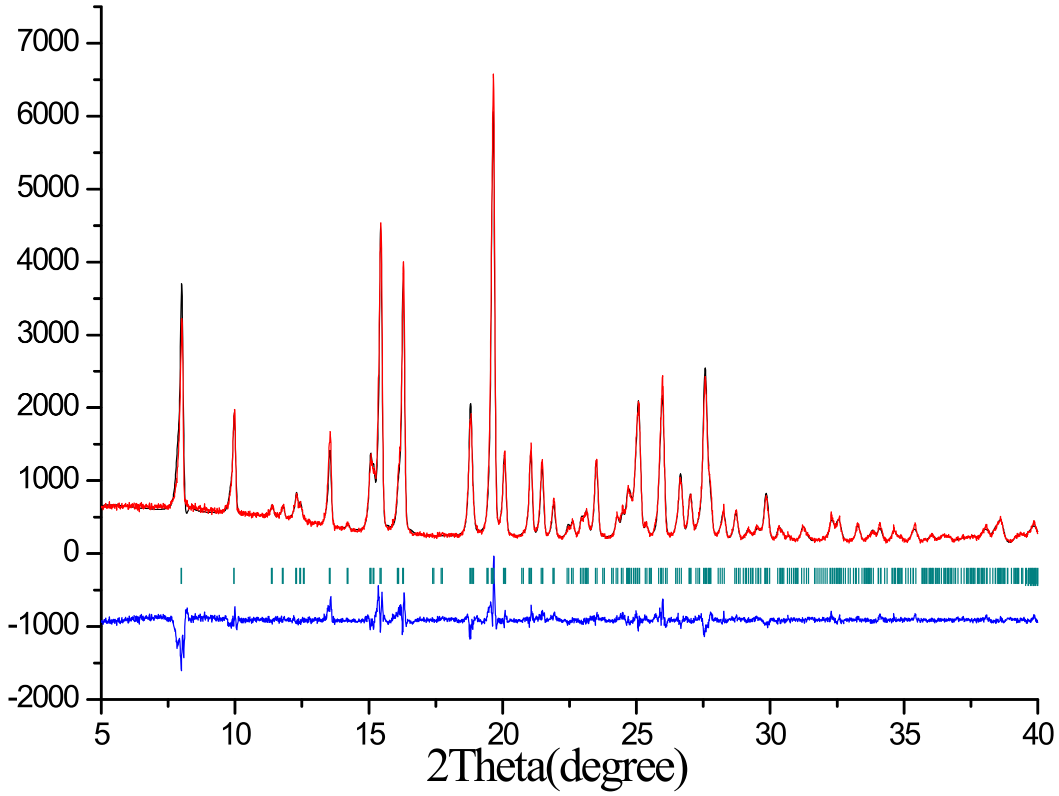

Figure S2 Experimental PXRD pattern (red), Rietveld simulated PXRD pattern (black) and their difference profile (blue) of SMT-SAC salt. The observed reflections are also marked (darkcyan). Residual variances: *R*wp = 7.82%, *R*p = 5.94 %

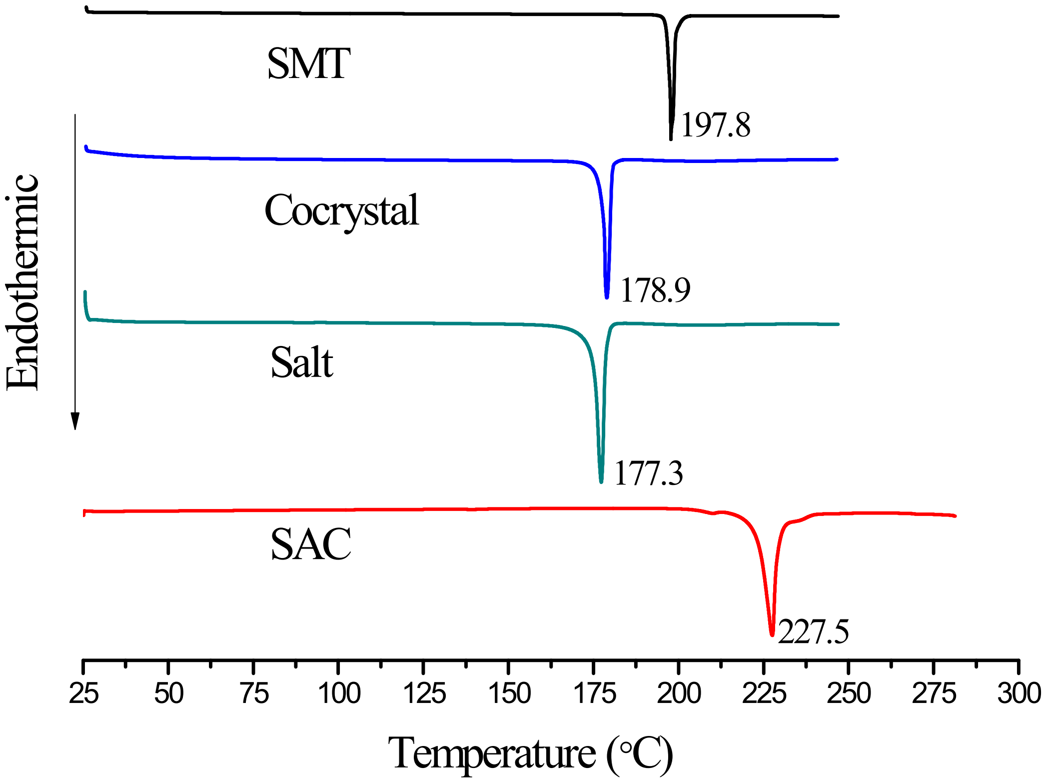

Figure S3 DSC curves of SMT, SAC, SMT-SAC salt and SMT-SAC cocrystal